

# On the frequency up-conversion mechanism due to a soft stopper by the example of an electrostatic kinetic energy harvester

Andrii Sokolov<sup>1</sup> , Dimitri Galayko<sup>2,3</sup>, Philippe Basset<sup>4</sup> and Elena Blokhina<sup>1</sup>

Journal of Intelligent Material Systems and Structures

1–10

© The Author(s) 2022



Article reuse guidelines:

sagepub.com/journals-permissions

DOI: 10.1177/1045389X221109258

journals.sagepub.com/home/jim



## Abstract

Micro- and meso-scale electrostatic energy harvesting systems have high efficiency at the higher-frequency part of the spectrum due to the natural frequencies of micro-structures lying over a range from hundreds of hertz to megahertz. However, many real-life applications related, in particular, to wearable systems, structural monitoring, or the Internet of Things, are characterized by low-frequency environmental forces. The main goal of this letter is to demonstrate that the placement of a stopper that limits the motion of the proof mass and causes soft impacts in an electrostatic kinetic energy harvester is responsible for an effect known as frequency up-conversion. This means that there is a significant response to “non-resonant” frequencies away from the natural frequency of the structure leading to effective energy conversion to the electrical domain. The concept summarizing this effect is presented and modeled, and an experiment carried out on a microscopic electrostatic harvester is presented to prove the concept.

## Keywords

Kinetic energy harvesting systems, MEMS, electrostatic KEHs, variable capacitors, frequency up-conversion

## 1. Introduction

One fundamental problem of the Internet of Things (IoT) technology is the electrical supply of network nodes. There are various ways to solve this problem—usage of chemical sources, solar energy, or mechanical vibrations. Kinetic energy harvesters generate electricity out of ambient vibrations utilizing the principle of a variable capacitor and can be useful in various applications including the powering of small sensors. The subject of this paper is Electrostatic Kinetic Energy Harvesters (eKEH) (Basset et al., 2016) where the proof mass is actuated by external acceleration and causes a variation of the capacitance of a pre-charged variable capacitor (see Figure 1).

For eKEH design, it is important to model the dynamic characteristics of the eKEH under different external excitation parameters to understand what are the most efficient operating conditions. One of the main characteristics of such devices is the output power versus the external actuation frequency, which is obtained when the external sinusoidal acceleration amplitude  $A_{\text{ext}}$  is fixed and the frequency  $f_{\text{ext}}$  is swept (Lu et al., 2015, 2016). It is usually desired to obtain a response

(high amplitude of the proof mass motion and hence the power converted to the electrical domain) over the widest possible range of external frequencies, and, in particular, at low frequencies (0–50 Hz) corresponding to vibrations in real-life systems of interest or vibrations produced by human motion. The extension of the frequency bandwidth of a linear resonator is often done by introducing mechanical or electrical nonlinearity (Blokhina et al., 2012; O’Riordan et al., 2015) or adding stopper elements (as shown in Figure 1) that limits the amplitude of the oscillations. However, the latter usually results in a “hardening” effect and extends the

<sup>1</sup>School of Electrical and Electronic Engineering, University College Dublin, Dublin, Ireland

<sup>2</sup>CNRS, LIP6, Sorbonne Université, Paris, France

<sup>3</sup>Centre for Nanoscience and Nanotechnology, Université Paris-Saclay – CNRS, Palaiseau, France

<sup>4</sup>ESYCOM, Univ Gustave Eiffel, CNRS, CNAM, ESIEE Paris, Noisy-le-Grand, France

### Corresponding author:

Andrii Sokolov, School of Electrical and Electronic Engineering, University College Dublin, Office 331, Belfield, Dublin 4, D04V1W8, Ireland.  
Email: andrii.sokolov@equall.com

resonator bandwidth to higher frequencies rather than to lower frequencies.

It has been reported that a significant growth of the converted power is observed at lower frequencies in harvesters with some particular configurations of stoppers or the proof mass with a cavity. The effect is known in the literature as frequency up-conversion. Since the first observation of this effect, there have been attempt to explain and quantify it, as well as to improve the design of the devices to enhance frequency up-conversion (Abedini and Wang, 2019; Fu and Yeatman, 2019; Guo et al., 2020; Jung and Yun, 2010; Kulah and Najafi, 2008; Lensvelt et al., 2020; Li et al., 2019, 2020, 2020; Naito and Uenishi, 2019; Speciale et al., 2020; Vysotskyi et al., 2016; Zhang et al., 2018; Zorlu et al., 2011).

The most representative and simple system for the modeling and design of a harvester with frequency up-conversion is a device with electromagnetic coupling. For this reason, some models of the frequency up-conversion effect have been attempted on this type of harvesters. The explanation of the effect is as follows. According to Faraday's Law, the current generated in the coil is proportional to the velocity of the proof-mass (Jung and Yun, 2010; Kulah and Najafi, 2008; Zorlu et al., 2011). In such a system, the conversion of energy at low-frequencies happens because of the collision of the proof-mass with a stopper. This produces an additional oscillation at the natural frequency of the resonator that is higher than the external excitation frequency.

With respect to other transduction mechanisms, a typical eKEH displays much more complicated dynamics because the charge induced on the plates of its variable capacitors has a strong influence on the waveforms in both, the electrical and mechanical domains. In this paper, we focus on the modeling of an eKEHs with a gap-closing variable capacitor as an example of a harvester whose nonlinearity arises in the electrical domain, as shown in Figure 1(a). Study (Li et al., 2020) presents an interesting mathematical model of the spring, electromechanical coupling and the hard-stopper force and predicts hardening effects in the investigated eKEH very well. However, the presented model does not explain in detail the frequency up-conversion occurring in the system.

There are more studies investigating the influence of the stoppers and addressing the bandwidth extension toward higher frequencies (the Duffing effect), but not the appearance of an enhanced low-frequency response (Ibrahim et al., 2018; Mahmoud et al., 2017).

This brief is focused on the quantitative investigation of the frequency up-conversion effect in a harvester with electrostatic transduction and nonlinearity in the electrical domain. Our aim is to propose a concise and accurate model that will not only explain why the effect

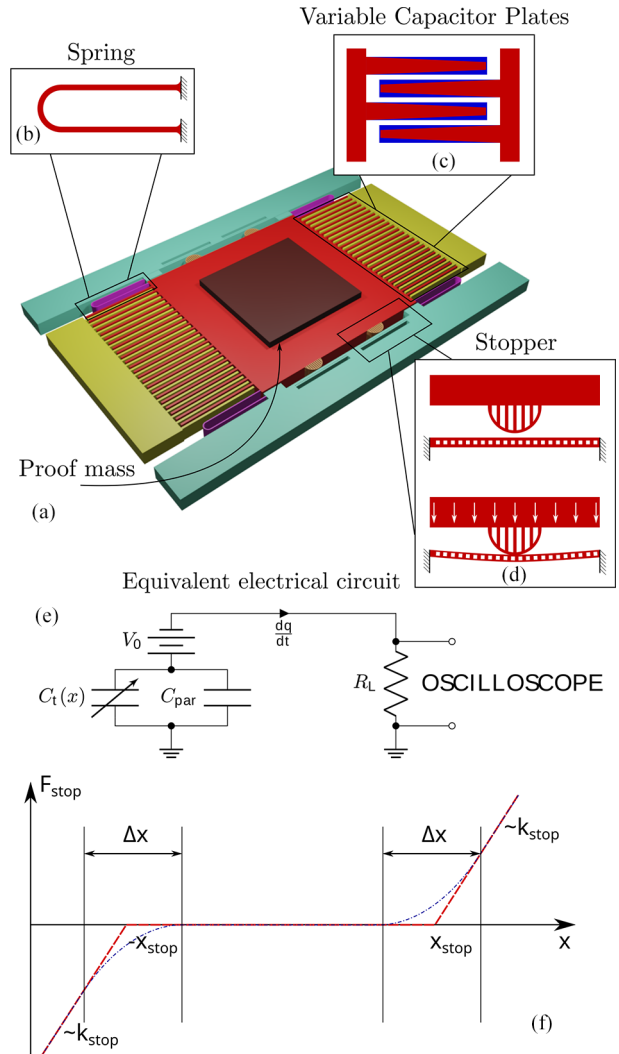


**Figure 1.** The schematic diagram presenting the structure of the electrostatic energy harvester under study in this paper constructed from the physical layout of the device. (a) General view of the structure. (b) 2D design of the linear spring. (c) The blue bars shows an initial layout of the variable capacitor. The red bars demonstrates an over-etching effect. (d) The elastic stopper, loaded and unloaded. (e) Basic electric conditioning circuit connected to the measurement equipment. (f) The stopper force versus coordinates: red dashed line is for the hard-stopper, blue dash-dot line is for the soft-stopper,  $\Delta x$  is the transient region.

happens but also will allow us to simulate the characteristic of a harvester in a predictive manner. To our knowledge, such a model is not discussed in the literature despite the fact that frequency up-converting is known.

The structure of the paper is as follows. Section II of the letter presents the statement of the problem that is formulated as a lumped model containing ordinary differential equations describing the mechanical and electrical domains. Section III briefly outlines the finite-element-method modeling of the system capacitance.

**Table 1.** Parameters extracted from the simulations.

Measured	Proof mass, $m$	$59 \times 10^{-6}$	kg
Fitted, using $a_{\text{ext}} = 0.5g$	Driving spring stiffness, $k$	18	N/m
Fitted, using $a_{\text{ext}} = 0.5g$	Quality factor, $Q$	13.5	
Measured	Stopper stiffness, $k_{\text{stop}}$	$2.5 \times 10^4$	N/m
Fitted using all data sets	Stopper quality factor, $Q_{\text{stop}}$	0.7	
Measured ( $d_{\text{stop}} - \Delta x$ )	Distance to the stopper, $d_{\text{stop}}$	$47.5 \times 10^{-6}$	m
Fitted using all data sets	Transient region, $\Delta x$	$10 \times 10^{-6}$	m
Measured	Load Resistance, $R_L$	$6.65 \times 10^6$	Ohm
Measured	Equilibrium Capacitance, $C_0$	$3.2 \times 10^{-12}$	F
Measured	Parasitic Capacitance, $C_{\text{par}}$	$28.0 \times 10^{-12}$	F
Measured with over-etching effect	Limit distance between plates, $d_{\text{lim}}$	$55.6 \times 10^{-6}$	m

Section IV presents the description of the experiment, experimental results, the technique to extract parameters and the comparison. In the Conclusions section, we discuss the novelty of the results and the advantage to use soft stoppers.

## 2. Statement of the problem

It is considered that frequency up-conversion is an effect when the resonator of a kinetic energy harvester exhibits high-power mode when the external excitation applied is at low frequency. This usually occurs due to collisions with stoppers or other collision related effects. To describe this phenomenon, we built a lumped model of the electrostatic energy harvester with a stopper based on the physical geometry. As the example here, we test the device whose fabrication is described in detail in Lu et al., 2015. The parameters of the device are given in Table 1.

Lumped models are a very common model of choice for MEMS resonators and kinetic energy harvesters based on them (Ibrahim et al., 2018; Mahmoud et al., 2017). For the device under study in this paper, we proposed a lumped model that includes the following forces:

$$m\ddot{x} = -kx - c\dot{x} + f_{\text{stop}}(x) + f_{\text{trans}}(x, q) - mA_{\text{ext}} \cos(2\pi f_{\text{ext}}t). \quad (1)$$

Here  $x$  is the displacement of the variable capacitor,  $m$  is the proof mass,  $k$  is the spring elasticity coefficient,  $c$  is the air damping coefficient evaluated from the quality factor of the system  $c = \sqrt{mk}/Q$ ,  $A_{\text{ext}}$  and  $f_{\text{ext}}$  are the external acceleration and external frequency respectively.

The motion of the resonators in kinetic energy harvesters are usually limited by stoppers. One can classify stoppers as hard or soft. For example, the effect of a hard stopper placed symmetrically on the both sides of the resonator can be modeled by an piece-wise function  $f_{\text{stop}}(x)$ :

$$f_{\text{stop}}(x) = \begin{cases} 0 & |x| < d_{\text{stop}}, \\ -\text{sign}(x - d_{\text{stop}}) \cdot k_{\text{stop}}(|x| - d_{\text{stop}}) + c_{\text{stop}}\dot{x} & |x| \geq d_{\text{stop}}, \end{cases} \quad (2)$$

Here,  $\text{sign}(x)$  is the signum function,  $d_{\text{stop}}$  is the stopper position,  $c_{\text{stop}}$  is the linear damping coefficient related to the collision process,  $k_{\text{stop}}$  is the stopper stiffness, which is considered to be much higher than the stiffness of the resonator  $k_{\text{stop}} \gg k$ . Note that the piece-wise function has a singularity in the first derivative at the switch-point that may cause instability in the ODE solver.

With respect to the soft stopper, its stiffness has a transient region and a wide region of response with respect to the relative displacement of the resonator. Its model is as following:

$$f_{\text{stop}}(x) = \begin{cases} -k_{\text{stop}}(x - d_{\text{stop}}), & x > (d_{\text{stop}} + \Delta x/2), \\ -\frac{k_{\text{stop}}}{2\Delta x} \left[ x^2 - (2d_{\text{stop}} - \Delta x)x + \frac{(2d_{\text{stop}} - \Delta x)^2}{4} \right], & x > (d_{\text{stop}} - \Delta x/2) \\ 0, & x \leq (d_{\text{stop}} + \Delta x/2), \\ & x > (-d_{\text{stop}} + \Delta x/2) \\ & x \leq (d_{\text{stop}} - \Delta x/2), \\ \frac{k_{\text{stop}}}{2\Delta x} \left[ x^2 + (2d_{\text{stop}} - \Delta x)x + \frac{(2d_{\text{stop}} - \Delta x)^2}{4} \right], & x > (-d_{\text{stop}} - \Delta x/2) \\ & x \leq (-d_{\text{stop}} + \Delta x/2), \\ -k_{\text{stop}}(x + d_{\text{stop}}), & x \leq (-d_{\text{stop}} - \Delta x/2). \end{cases} \quad (3)$$

The parameters of the stopper are to be reconstructed from measured data. The softness of a stopper is regulated by the width of the  $\Delta x$  region.

The transducer force  $f_{\text{trans}}(x, q)$  has an electrostatic origin and therefore it depends on the charge  $q$  on the plates of the variable capacitor. To know the charge, the electrical setup of the experiment needs to be modeled. In this case, the transducer is biased by an electret layer, and eventually, a DC voltage source may be added to modify the biasing. The electrical setup is presented in Figure 1(e). The transducer is loaded with a resistance: that allows one to measure the converted power by measuring the voltage on the resistance. Thus, using the Kirchhoff Voltage Law (KVL) we can write the differential equation for the charge in the circuit:

$$R_L \frac{dq}{dt} + \frac{q}{(C_t(x) + C_{\text{par}})} = V_0. \quad (4)$$

Here  $R_L$  is the load resistance and  $V_0$  is the total bias voltage (electret plus external one). The transducer force  $f_{\text{trans}}(x, q)$  and the variable capacitance  $C_t(x)$  can be modeled as an approximation of the ideal flat variable capacitor (the electric field between plates assumed uniform), however, it needs to be refined using more accurate Finite Element Method (FEM) simulations.

Up until this point, the basic component of the model are general. In the next sections, we will show that adding the accurate modeling of the capacitance and understanding the nonlinear effects produced by the stopper will allow us to explain the *physics* of frequency up-conversion (qualitatively and quantitatively) through the generation of higher harmonics.

### 3. Verification of 1D model using finite element simulations

For the model of the variable capacitor, we use the ideal gap-closing approximation. The following expression connects the variable capacitance  $C_t(x)$  and the displacement  $x$  of the proof mass:

$$C_t(x) = \frac{2C_0 d_{\text{lim}}^2}{d_{\text{lim}}^2 - x^2}, \quad (5)$$

where  $C_0$  is the capacitance of the system in the equilibrium state and  $d_{\text{lim}}$  is the default (rest) distance between two neighbor plates as shown in Figure 2(a). The expression for the transducer force can be written then as follows:

$$f_{\text{trans}}(x, q) = \frac{1}{2} \frac{q^2}{C_t^2(x)} \frac{dC_t(x)}{dx}. \quad (6)$$

However, one has to note that the expression above does not take into account the non-uniformity of the

electric field at the edges of the plates and the effects associated with over-etching during the manufacturing of the device (see Figure 1(c)). For this reason, we employ a 3D model of the variable capacitor of the studied device using the layout and over-etching of the plates effects (Figure 2(b)). Using a FEM Poisson equation solver (COMSOL Multiphysics), we calculate the 3D electric potential distribution, variable capacitance of the structure and the electrostatic force acting on it (Figure 2(c) and (d)).

The FEM solver corroborated the hypothesis that the over-etching effect causes only minor changes in the magnitude of  $C_0$ ,  $d_{\text{lim}}$  and in the overall expression for the transducer force. Hence, the ideal capacitor approximation we started with is valid in this case. We can use these expressions in equations (1) and (4). However, we allow ourselves to vary  $C_0$  and  $d_{\text{lim}}$  within 10% – 15% of the reference values since we assume that some other effects (during the manufacturing or elsewhere) can impact the device.

### 4. Results: Experimental observation of frequency up-conversion and its analysis

The photo of the experimental set up is shown in Figure 3. The experiment consisted of measuring the power dissipated across the load resistor (see Figure 1(e)). It was then converted into the energy per cycle of oscillations. The forward and backward frequency sweeps were recorded over a frequency range from 0 to 500 Hz. The electrostatic transducer (variable capacitor) was biased either by an electret of 21 V or by the electret (21 V) and an additional source of 25 V. Different harmonic accelerations were applied: weak (0.5 g), intermediate (1 g) and strong (2 g). The measurements are visualized in Figure 4.

For the studied device, Table 1 summarizes what parameters are known or measured directly (i.e. mass  $m$ , load resistance  $R_L$ , etc) and what parameters have been extracted from the experimental data (i.e. stopper  $Q$ -factor, etc). We note that some of them ( $m$ ,  $R_L$ ,  $C_0$ ) can be measured with very high precision, while other parameters ( $d_{\text{stop}}$ ,  $d_{\text{lim}}$ ) have reliable reference values but can vary within 5%–10% due to the fabrication effects (Lu et al., 2016; Vysotskyi, 2018). The linear resonator parameters  $k$  and  $Q$  have been extracted using the lowest excitation acceleration amplitude of 0.5g. The stoppers stiffness can be estimated using the approach for a clumped-clumped beam. Finally, the stoppers  $Q$ -factor is very difficult to predict since these characteristics can be affected by nonlinear effects such as squeezed-film damping. Thus, these parameters were initially chosen randomly, and then fitted using all acceleration and bias-voltages data sets as is described later in this section.

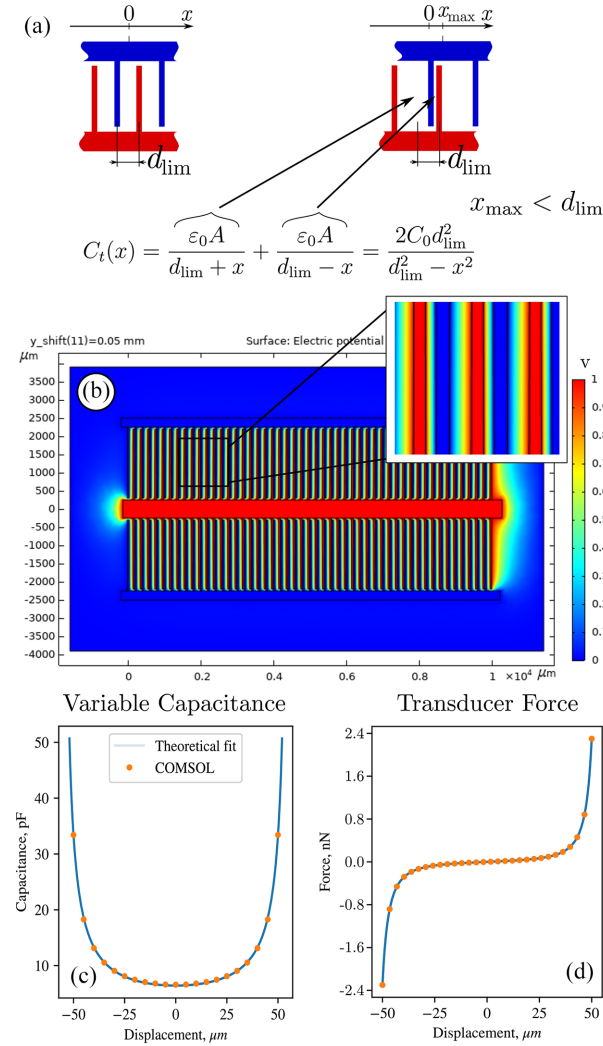


**Figure 2.** Capacitance and transducer force calculation. (a) The principle of the gap-closing capacitor and the analytical formula describing it. (b) Finite Element Method simulations of the electric potential distribution due to the variable capacitor plates at a fixed potential difference of 1V. (c) Capacitance versus displacement: orange circles show the results of the FEM simulations while the blue line shows the function fitted with (5). (d) Transducer force versus displacement: orange circles show the results of the FEM simulations while the blue line shows the function fitted with (6).

As was mentioned in the Introduction, gap-closing eKEHs often display complex dynamics depending on many factors, and not all of them are possible to measure (See Table 1). Moreover, in this paper we focus on the low-frequency region of forced oscillations that may display some (not significant) disagreement with experimental data. However, the proposed model allows one both options, to model the frequency up-conversion effect and the hardening of the resonance curve.

The methodology of this study is based on the numerical modeling and optimization of the equations outlined in previous section and comparison of the

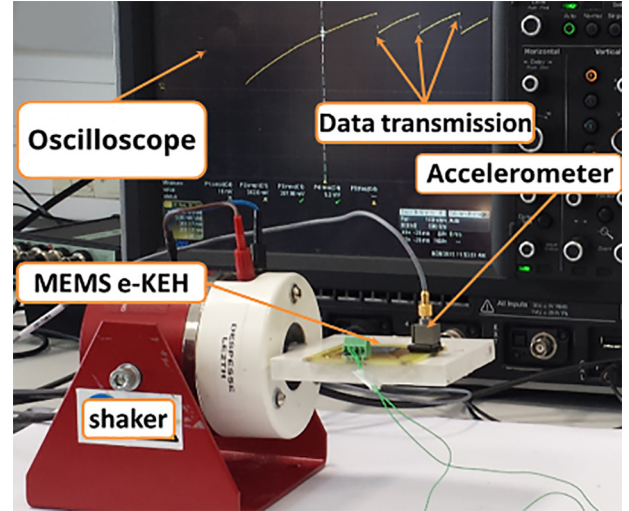


**Figure 3.** The experimental setup: an electrostatic KEH is set into motion by a shaker. The acceleration (amplitude and frequency) is controlled by an external accelerometer and feedback loop. The energy generated per cycle ( $i$  and  $V$ ) is recorded by a digital oscilloscope.

simulated parameter sweeps with the experiment. In order to perform the optimization and comparison, we applied numerical integration with controlled accuracy (using the *boost-odeint* library (Ahnert and Mulansky, 2020)) to the system of equations (1), (4) with known functions (5) and (6) and obtained the  $x(t)$  and  $q(t)$  waveforms for given  $f_{\text{ext}}$  and  $A_{\text{ext}}$ . Since the frequency sweeps (aka resonance curves) require steady-state, we analyze the waveforms of the last 10 of total 50 cycles of oscillations.

The amplitude of oscillations can be calculated as  $(x_{\text{max}} - x_{\text{min}})/2$ , and the energy generated per cycle can be found as follows:

$$W = - \int_0^{T_{\text{ext}}} f_{\text{trans}}[x(t), q(t)] \dot{x}(t) dt, \quad (7)$$

where  $T_{\text{ext}}$  is the period of the driving (external) acceleration. This technique allowed us to simulate the frequency sweeps based on the model and compare them with the experimental ones (Figure 4).

The mathematical model of the studied KEH, although formulated in a general form, allows one to obtain some deep understanding of the factors that affect the generation of energy at different external frequencies, in particular, in the sub-resonance region where frequency up-conversion takes place. We would like to highlight again that this effect (frequency up-conversion) was reported in the literature, however to the knowledge of the authors there is no quantitative model explaining its physics.

The coordinate  $x(t)$ , velocity component  $\dot{x}(t)$  and charge  $q(t)$  waveforms were obtained from the model in

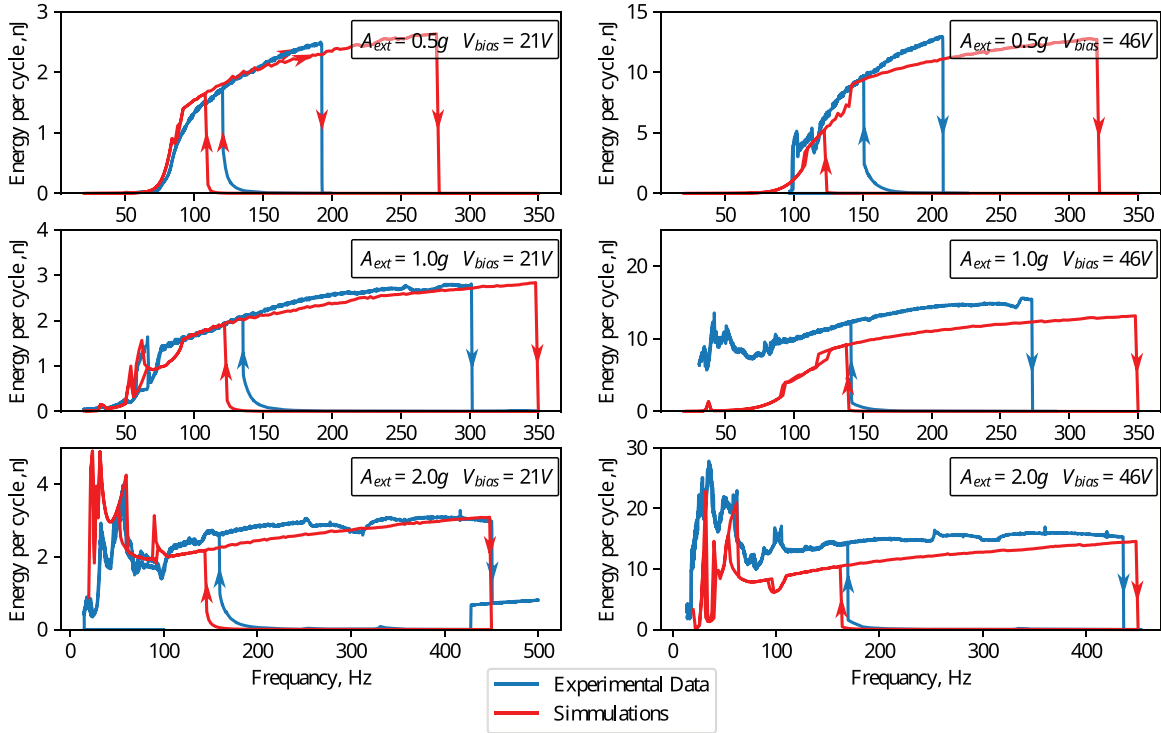


**Figure 4.** Matching of the experimental data with the simulation results. The blue lines correspond to the measured energy converted per oscillation cycle on the device. The red lines correspond to the simulation results. Note that the variable capacitor is pre-charged by the electret layer with voltage 21V (left column) or have a source of 25 V connected to it in addition to the electret (right column).

steady-state at different external excitation parameters ( $A_{ext}, f_{ext}$ ), and their spectra in the frequency domain (FFTs) calculated. The FFTs allow us to decompose the signal excited by the acceleration  $A_{ext} \cos(2\pi f_{ext}t)$  in form:

$$x(t) = A_0 + \sum_n A_n \cos(2\pi n f_{ext}t + \phi_i), \quad (8)$$

where  $n$  is an integer. We are mostly interested in the first five harmonics of the driving frequency  $f_{ext}$ . The coordinate and velocity waveforms do not have a DC offset  $A_0$ , and have only odd non-zero harmonics. It is easy to see from (5) that for the single transition of displacement from minimum to maximum  $x_{min} \rightarrow x_{max}$ , the capacitance  $C_t(x)$  displays a full cycle  $C_{max} \rightarrow C_{min} \rightarrow C_{max}$ . For this reason, the variable capacitor charge waveform  $q(t)$  has only even non-zero harmonics.

Figure 5 illustrates that the frequency up-conversion effect is due to higher harmonics generated by the KEH resonator. The graph at the center of the figure shows a simulated frequency sweep (forward and backward branches) with a clear up-conversion region for the frequencies below the linear resonance one. The heat map on top of the figure shows the relative magnitude (in dB) of higher harmonics  $A_n$  ( $n = 1, 2, \dots$ ) generated by the KEH at a given frequency  $f_{ext}$  of external driving for

the forward branch. (The same heat map for the backward branch is shown at the bottom of the figure.) It is clearly seen that soft impact with the stopper leads to multiple higher harmonics, and these harmonics decay significantly when the system is driven into the region of hard impact with the stopper.

These concept is further expanded in Figure 6 where the distribution of energy per cycle of oscillations across higher harmonics is presented. As an example, we take the same case as shown in Figure 5:  $A_{ext} = 2g$  and  $V_0 = 21$  V. The blue colored area encodes the energy generated by the first (fundamental) oscillation harmonic. It demonstrates that the fundamental harmonic behaves in a “conventional” nonlinear way with a hardening spring effect when the KEH is driven into hard impact with the stopper. The orange and the green areas show the energy generated by the third and the fifth harmonics respectively. Analyzing those graphs, it is easy to see the origin of the frequency up-conversion: it occurs when the bumper of the resonator softly collides with the stopper and causes the system to oscillate on high oscillation modes (see samples of waveforms). When the bumpers start to collide with the stoppers strongly, the waveform becomes “triangular” and, at some point, the fundamental harmonic dominates. The red area shows the rest of the generated energy, and the dashed line shows the linear natural frequency of the

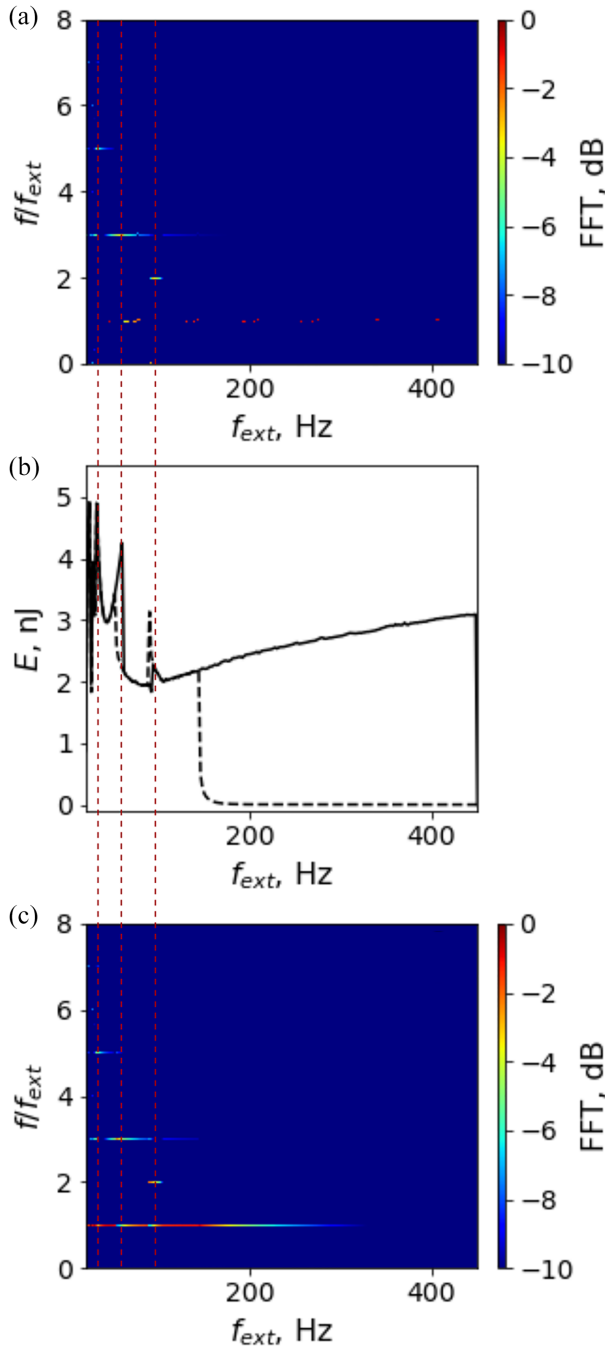


**Figure 5.** Analysis of the forward and backward branches of the system under the bias voltage  $V_0 = 21V$  and an external acceleration  $A_{ext} = 2g$ . The x-axis of all three graphs is the driving frequency. The middle graph (b) is the energy per cycle with frequency up-conversion highlighted area. The upper and bottom heat maps (a and c) show the balance between harmonics on a different driving frequencies for the forward and backward resonance branches respectively.

system ( $f_{linear}$ ). It is easy to see that with the frequency up-conversion effect, the high power is generated at the frequencies lower than the natural one.

Figure 6 provides further explanation on the frequency up-conversion effect from the stand-point of the dynamics of the harvester's resonator (obtained by solving the correspondent set of equations). The frequency sweeps, containing the forward and backward branches of the energy per cycle and amplitude, are shown at the top of the figure. The points of interest  $A$ ,  $B$ ,  $C$ ,  $D$ , and  $E$  are added, with the points  $A$ ,  $B$ ,  $C$ , and  $D$  sampled in the region of frequency up-conversion and point  $E$  taken in the region of the stable collision of the resonator with the stopper. The first and second columns visualize the displacement as a function of time and the displacement in the form of a phase portrait (in the state space spanned by  $x(t)$  and  $\dot{x}(t)$ ). The third column presents the interplay between resonator's spring and the stopper force, showing a significant increase in the stopper force at the instances of collisions. The fourth column shows the Fast Fourier Transforms (FFT) of the displacement waveform  $x(t)$  to highlight the generation of higher harmonics that become dominant in the regime of resonator-stopper collisions (frequency up-conversion).

One should note that the peaks in the frequency sweep (points  $B$  and  $D$ ) correspond to the maximal generation of the third and fifth harmonics due to collisions. For comparison, point  $E$  is taken in the region of regular resonator-stopper collisions (producing a well-known hardening effect on the frequency sweep). At this point, as one can see, higher harmonics are still generated (since the waveform  $x(t)$  is clearly nonlinear), but the fundamental harmonic is dominant. It should also be noted that in case  $E$  (no frequency up-conversion), the stopper force becomes significant compared to cases  $A$ - $D$  (with frequency up-conversion), implying it is soft collisions with the stopper that are responsible for frequency up-conversion and amplitude enhancement.

## 5. Conclusions

This brief paper is dedicated to an explanation into the frequency up-conversion effect based on a quantitative model. We use a compact lumped model of a electrostatic kinetic energy harvester with a (soft) stopper and a basic conditioning circuit. Using FEM simulations, we proved that a simple expression for the variable capacitance and the transducer force are applicable for the investigated harvester. Using that model we showed that the collisions between the proof-mass and the stoppers are causing higher harmonic oscillations and therefore causes frequency up-conversion in this system.

The key points are as follows:

- Frequency up-conversion is observed in a harvester with a linear resonator and a soft stopper

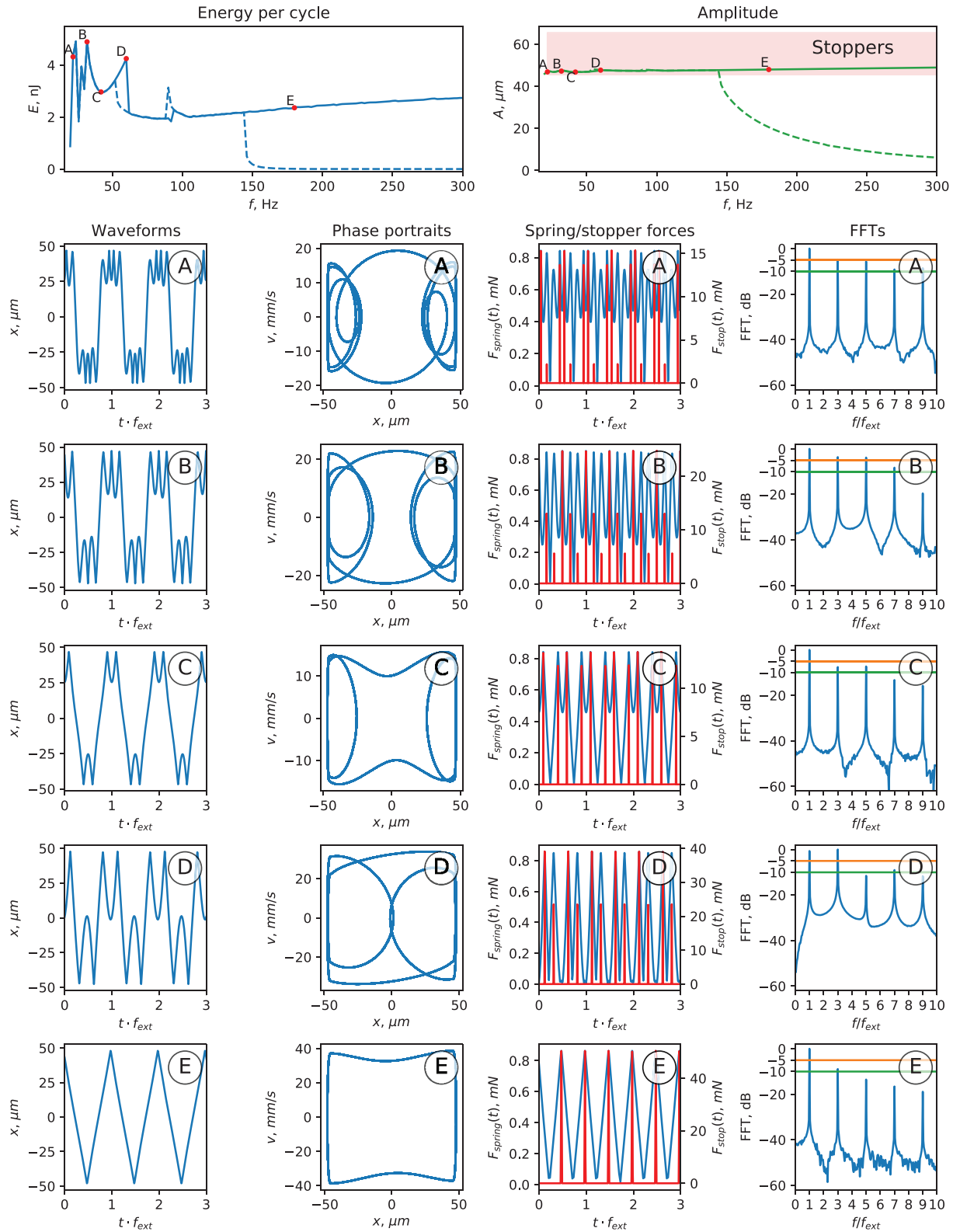


**Figure 6.** Analysis of the forward and backward branches of the system's frequency sweep under the bias voltage  $V_0 = 21\text{V}$  and an external acceleration of  $A_{\text{ext}} = 2g$ . Two top graphs are the resonance curves of the KEH with characteristic points B, C, D, and E. The top-left graph is the energy per cycle versus frequency, and the top-right one is the amplitude versus frequency (with transient region shown). Then each row of the graph show properties of a given characteristic point. The first column demonstrate displacement wave-forms, the second—phase portraits, the third one allow one to see the evolution of both  $F_{\text{spring}}$  and  $F_{\text{stop}}$ . The last column show the Fourier transform of each waveform with two horizontal lines on  $-5$  and  $-10$  dB.



when the frequency of the external oscillations is below that of linear resonance.

- Frequency up-conversion occurs when the linear resonator experiences a very soft impact with the stopper and is explained by the generation of higher oscillations harmonics. The harvester generated as increased converted power.
- When the KEH is driven into hard-impact mode, higher harmonics decay. The converted power increases as is similar to conventional hardening nonlinearity cases.
- Soft stopper may be particularly useful in this case as it is important to keep the KEH oscillators in the mode of soft bouncing. Soft stoppers can be modeled using the approximation of the smoothed stopper force with relatively wide transient region
- While frequency up-conversion was observed and reported in other systems with impact, we provide a compact model and physics explanation of this effect.


### Declaration of conflicting interests

The authors declared no potential conflicts of interest with respect to the research, authorship, and/or publication of this article.

### Funding

The authors disclosed receipt of the following financial support for the research, authorship, and/or publication of this article: This document is the results of the research project funded by Science Foundation Ireland under grant 13/RC/2077

### ORCID iD

Andrii Sokolov  <https://orcid.org/0000-0001-5655-115X>

### References

- Abedini A and Wang F (2019) Energy harvesting of a frequency up-conversion piezoelectric harvester with controlled impact. *The European Physical Journal Special Topics* 228(6): 1459–1474.
- Ahnert K and Mulansky M (2020) Boost numeric odeint. Available at: [https://www.boost.org/doc/libs/1\\_73\\_0/libs/numeric/odeint/doc/html/index.html](https://www.boost.org/doc/libs/1_73_0/libs/numeric/odeint/doc/html/index.html)
- Basset P, Blokhina E and Galayko D (2016) *Electrostatic Kinetic Energy Harvesting*. Hoboken, NJ: John Wiley and Sons.
- Blokhina E, Galayko D, Harte P, et al. (2012) Limit on converted power in resonant electrostatic vibration energy harvesters. *Applied Physics Letters* 101(17): 173904.
- Fu H and Yeatman EM (2019) Rotational energy harvesting using bi-stability and frequency up-conversion for low-power sensing applications: Theoretical modelling and experimental validation. *Mechanical Systems and Signal Processing* 125: 229–244.
- Guo X, Zhang Y, Fan K, et al. (2020) A comprehensive study of non-linear air damping and pull-in effects on the electrostatic energy harvesters. *Energy Conversion and Management* 203: 112264.
- Ibrahim A, Ramini A and Towfighian S (2018) Experimental and theoretical investigation of an impact vibration harvester with triboelectric transduction. *Journal of Sound and Vibration* 416: 111–124.
- Jung SM and Yun KS (2010) Energy-harvesting device with mechanical frequency-up conversion mechanism for increased power efficiency and wideband operation. *Applied Physics Letters* 96(11): 111906.
- Kulah H and Najafi K (2008) Energy scavenging from low-frequency vibrations by using frequency up-conversion for wireless sensor applications. *IEEE Sensors Journal* 8(3): 261–268.
- Lensvelt R, Fey RHB, Mestrom RMC, et al. (2020) Design and numerical analysis of an electrostatic energy harvester with impact for frequency up-conversion. *Journal of Computational and Nonlinear Dynamics* 15(5): 051005.
- Li J, Tichy J and Borca-Tasciuc DA (2020) A predictive model for electrostatic energy harvesters with impact-based frequency up-conversion. *Journal of Micromechanics and Microengineering* 30(12): 125012.
- Li J, Tong X, Oxaal J, et al. (2019) Investigation of parallel-connected mems electrostatic energy harvesters for enhancing output power over a wide frequency range. *Journal of Micromechanics and Microengineering* 29(9): 094001.
- Li P, Xu N and Gao C (2020) A multi-mechanisms composite frequency up-conversion energy harvester. *International Journal of Precision Engineering and Manufacturing* 21: 1781.
- Lu Y, Cottone F, Boisseau S, et al. (2015) A nonlinear mems electrostatic kinetic energy harvester for human-powered biomedical devices. *Applied Physics Letters* 107(25): 253902.
- Lu Y, O’Riordan E, Cottone F, et al. (2016) A batch-fabricated electret-biased wideband MEMS vibration energy harvester with frequency-up conversion behavior powering a UHF wireless sensor node. *Journal of Micromechanics and Microengineering* 26(12): 124004.
- Mahmoud MAE, Abdel-Rahman EM, Mansour RR, et al. (2017) Out-of-plane continuous electrostatic micro-power generators. *Sensors* 17(4): 877.
- Naito Y and Uenishi K (2019) Electrostatic mems vibration energy harvesters inside of tire treads. *Sensors* 19(4): 890.
- O’Riordan E, Dudka A, Galayko D, et al. (2015) Capacitive energy conversion with circuits implementing a rectangular charge-voltage cycle part 2: Electromechanical and non-linear analysis. *IEEE Transactions on Circuits and Systems I Regular Papers* 62(11): 2664–2673.
- Speciale A, Ardito R, Baù M, et al. (2020) Snap-through buckling mechanism for frequency-up conversion in piezoelectric energy harvesting. *Applied Sciences* 10(10): 3614.
- Vysotskyi B (2018) *Electrostatic MEMS vibrational energy harvester with large bandwidth for biomedical applications*. PhD Thesis, Université Paris Saclay (COMUE), Paris, France.

- Vysotskyi B, Parrain F, Lefeuvre E, et al. (2016) Design and simulation of bistable microsystem with frequency-up conversion effect for electrostatic energy harvesting. *Journal of Physics Conference Series* 757: 012007.
- Zhang Y, Wang T, Luo A, et al. (2018) Micro electrostatic energy harvester with both broad bandwidth and high normalized power density. *Applied Energy* 212: 362–371.
- Zorlu Ö, Topal ET and Kulah H (2011) A vibration-based electromagnetic energy harvester using mechanical frequency up-conversion method. *IEEE Sensors Journal* 11(2): 481–488.